



FIRST EXOPLANET AND DISK RESULTS WITH THE PALM-3000 ADAPTIVE OPTICS SYSTEM

Rick Burruss^{1a}, Sasha Hinkley³, Matthew Wahl⁴, Jonas Kuhn¹, Eric Cady¹, Richard Dekany²,
Bertrand Mennesson¹, Stanimir Metchev⁴, Ben Oppenheimer⁵, Rahul Patel⁴, Jennifer Roberts¹,
Eugene Serabyn¹, J. Chris Shelton¹, Jonathan Tesch¹, Gautam Vasisht¹

¹Jet Propulsion Laboratory, California Institute of Technology, Pasadena, CA, USA

²California Institute of Technology, Caltech Optical Observatories, Pasadena CA, USA

³California Institute of Technology, Department of Astronomy, Pasadena CA, USA

⁴Stony Brook University, Department of Astronomy, Stony Brook, NY, USA

⁵American Museum of Natural History, Department of Astrophysics, New York, NY, USA

Abstract. We describe the status of the PALM-3000 adaptive optics facility instrument for the Hale telescope at Palomar Observatory. Since first light in June 2011, PALM-3000 has made significant advances in both performance and sensitivity. Using strehl ratio as our performance metric, we present results in 64x64 and 32x32 wavefront sensor pupil sampling modes on a range of guide stars from $m_v = 0$ to 16. We describe our automated reconstructor pipeline tool, which incorporates pupil illumination and an optimal-estimator Bayesian approach to boost faint guide star performance. We conclude by presenting initial high-contrast circumstellar disk results from the PHARO vector vortex coronagraph and exoplanet spectra from the P1640 integral field spectrograph.

1. Introduction

PALM-3000 is the second generation adaptive optics facility instrument for the Hale telescope at Palomar Observatory. It is optimized for high-contrast studies of exoplanets and debris disks orbiting nearby bright stars when used with coronagraphic instrumentation, including the Palomar High-Angular Resolution Observer (PHARO), and the speckle-suppressing integral field spectrograph P1640. Three more instruments round out the PALM-3000 instrument suite; the Palomar Fiber Nuller (PFN), a near-infrared interferometric coronagraph; SWIFT, an I to Z band integral field spectrograph; and TMAS, a high speed visible imager [1].

PALM-3000 uses two Xinetics, Inc. deformable mirrors in a “woofer-tweeter” configuration to provide the optical phase corrections. The low order mirror is the original 349 actuator deformable mirror used in the first generation adaptive optics instrument at Palomar since 1999. The new high order mirror contains 3388 actuators, and is the largest format astronomical deformable mirror used on sky to date.

The PALM-3000 wavefront sensor is a Shack-Hartmann camera with three user-selectable pupil sampling modes; 64x64 subapertures = 8.3 cm per subaperture, 32x32 subapertures = 16.2 cm per subaperture, and 8x8 subapertures = 65 cm per subaperture (8x to be released in early 2014). Each frame taken by the sensor is sent to the PALM-3000 real-time computer (RTC) over a high-speed switch. The RTC is based on a GPU implementation of 16 NVIDIA 8800 GTX graphics cards hosted by eight dual-core Opteron PCs, each performing a vector matrix multiply on a subset of the data

^a email : Rick.S.Burruss@jpl.nasa.gov

frame. The eight PCs send the computed command subsets to a central servo PC, which assembles them into command vectors that are broadcast to the tip-tilt, low order, and high order adaptive mirrors.

The high actuator density in the PALM-3000 system requires an accurate reconstructor matrix in order to achieve robust closed-loop stability. In operation, the telescope pupil shifts slightly with respect to PALM-3000 as the telescope is moved from target to target, inducing a small but non-negligible shift of the amplitude function in the reconstruction matrix. As a result, we have implemented an automated reconstructor pipeline tool to measure the illumination function at each telescope position. We have also adopted a fully parameterized optimal-estimator Bayesian algorithm whereby reconstruction control is shifted from high to low spatial frequencies when observing on fainter targets. Nearly all of our on-sky data taken on stars fainter than 11th m_v show a noticeable performance boost when using the optimal-estimator parameters (Figure 1). Since first light in June 2011, the PALM-3000 team has made steady progress improving instrument performance on bright to faint guide stars, and we are planning to continue this effort in the near future as we work to release the 8x8 pupil sampling mode.

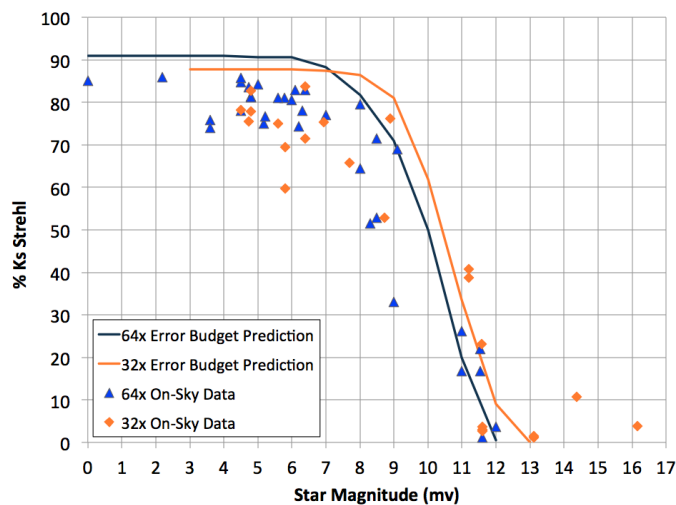


Figure 1: PALM-3000 error budget performance prediction curves for both 64x64 and 32x32 pupil sampling modes in median seeing conditions ($r_0 = 0.092$ meters) and wind speeds (8 meters / second) at zenith in the K-short band. 64x64 on-sky data points were taken over six observing nights between September 2012 to August 2013, and 32x32 on-sky data points were taken over three observing nights from March 2013 to August 2013. All of the on-sky data points were taken within 15° of zenith and after non-common path error calibration. The mean PALM-3000 64x strehl ratio on stars brighter than 8th m_v, over the course of the six nights is 80.4%.

2. PHARO Vector Vortex Coronagraphy

The Vector Vortex Coronagraph (VVC) [2] is a phase-based coronagraph installed in the PHARO science camera. As such it can theoretically access small inner working angles (down to the telescope diffraction limit) because phase masks are transparent, in particular at very small angles from the optical axis (unlike opaque masks). However, when observing from the ground, exquisite wavefront correction is necessary in order to take full advantage of this property. Consequently, our initial demonstrations of the VVC's performance used a well-corrected off-axis sub-aperture (WCS) of the Palomar primary mirror spanning only 1.5 meters of the full diameter, yielding very high Strehl ratios at K-band, providing a direct image of exoplanets separated by only two diffraction beamwidths from its central star [3]. As the PALM-3000 came on-line in 2011, providing accurate wavefront correction over the full 5.1 meter aperture, we started using an optimized VVC for the full telescope, hence benefiting from the increased sensitivity and angular resolution. Additional improvements are in the works, specifically to VVC manufacturing and design (specifically the ability to cope with the central obscuration of the telescope), as well as the introduction of a dedicated second-generation coronagraphic bench.

2.1. Direct Detection of Stellar Companions

As an example of high-contrast direct imaging performance currently enabled by PALM-3000, we present on-sky results obtained during two PHARO + VVC observing nights on November 4 and 5 2012 (UT). These nights were both characterized by relatively poor seeing conditions, typically oscillating between 1.5'' and 2'' measured in the visible band.

A first capability example is illustrated with direct imaging of the B9 star Kappa Andromedae (k And), which was recently shown to possess a dim, gravitationally bound companion (possibly close to the limit of planetary mass) at a projected separation of 55 AU (1.06'') [4]. We observed k And during the night of November 5 UT, 2012, in the narrow Br-gamma band to avoid saturation on the detector. We opted for a Reference Differential Imaging (RDI) data reduction strategy, and thus integrated 350 frames of 5.7 seconds each on k And, while interlacing them with 300 frames of 7.1 seconds on the calibrator star HD22173 every 50 frames or so, with rapid telescope slew in-between. This represents a total of roughly 30 minutes integration per star, but due to the poor seeing conditions we chose to discard several frames during the data reduction process, ending up with 126 quality frames (12 minutes) on k And, and 142 frames (17 minutes) on the calibrator HD22173.

Our IDL-based data reduction pipeline is quickly described as successive processing steps as follows: flat-fielding and sky subtraction, cosmic ray sigma-filtering, image registration, Principal Component Analysis (PCA) on the calibrator image stack to build a Karhounen-Loewe (KL) orthogonal basis of pseudo-images, target image stack projection on the KL basis, and photometry calibration on the residual image after KL projection using a set of acquired unobscured PSFs of k And. The Karhounen-Loewe Image Projection (KLIP) step is a direct implementation of the approach recently proposed by Soummer *et al* [5]. The resulting reduced image and the contrast plot are depicted in Figure 2, showing that k And B is easily detected at the 22σ level. Retrieved photometry vs. the primary star is $\Delta K_{\text{Br-g}} = 1.31 \cdot 10^{-4} \pm 1.5 \cdot 10^{-5}$ (9.7 ± 0.13 mag): this is 0.3 magnitudes brighter than the previously published ΔK_s value [4].

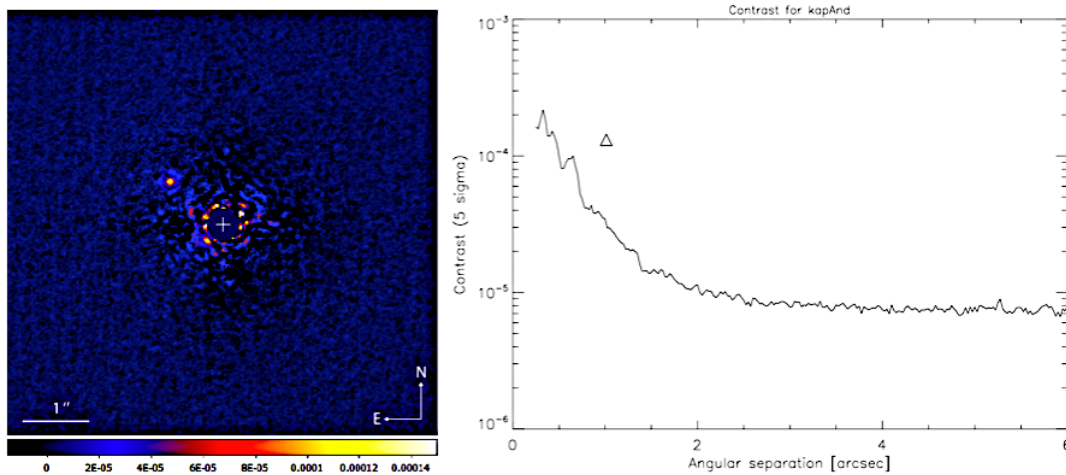


Figure 2: (Left) k And Br-gamma image after KLIP processing and photometry calibration. The white cross indicates primary star position and the inner $2.5 \lambda/D$ region is masked. (Right) 5σ contrast curve in function of separation, showing the achievable contrast under the current PALM-3000 and PHARO settings. The triangle represents the companion photometry, here corresponding to a 22σ detection level. (Note that a cone of azimuth angles $\pm 10^\circ$ away from the companion was excluded from the contrast plot computation to illustrate the true detectability level.)

In order to illustrate the current inner working angle performance of PHARO with the VVC, we also observed Epsilon Cephei (ϵ Cep) in K_s band during the night of November 4 UT, 2012. This F0 star is known to exhibit a $\Delta K_s \sim 2\%$ stellar companion at an angular separation of 300 mas, which was

discovered in 2010 using the same VVC technology but through the 1.5m WCS before PALM-3000 enabled full-aperture capabilities [6].

Here we integrated for 7 minutes on ϵ Cep, as well as 4.5 minutes on the RDI calibrator star HD213558, once again in non-optimal seeing conditions ($1.5''$). The final KLIP-reduced image of ϵ Cep is shown in Figure 3, demonstrating an effective inner working angle detection at less than $3\lambda/D$. The measured flux ratio of $\Delta K_s = 1.95 \cdot 10^{-2} \pm 2 \cdot 10^{-4}$ (4.3 ± 0.01 mag) is in excellent agreement with the 2010 WCS value of $\Delta K_s = 2 \cdot 10^{-2} \pm 5 \cdot 10^{-3}$. The detectability level of ϵ Cep b is at 10.8σ despite an estimated separation of 230 mas, corresponding to roughly $2.5 \lambda/D$.

2.2. Direct Detection of Circumstellar Disks

Images of the dusty debris disk around HD 141569 were obtained with the PALM-3000 adaptive optics system on the Hale telescope in June 2012. HD 141569 is an A0 type Herbig Ae star located at 99 ± 8 pc with an age of roughly 5 Myrs [7]. We used a hard-edge occulting mask located in PHARO's focal plane, and the VVC coronagraph for these observations.

Observations of a reference star, HD 142864, were also carried out so that accurate point spread function subtraction can be achieved. We integrated for 1 hour on target, in H and Ks bands, and 0.5 hours on the calibrator star. The data were analyzed using the Karhunen-Loeve Image Processing technique which performs principle component analysis. Our images (Figure 4) resolve the known two-ring structure of the disk, and are the most sensitive to date in the H and K bands.

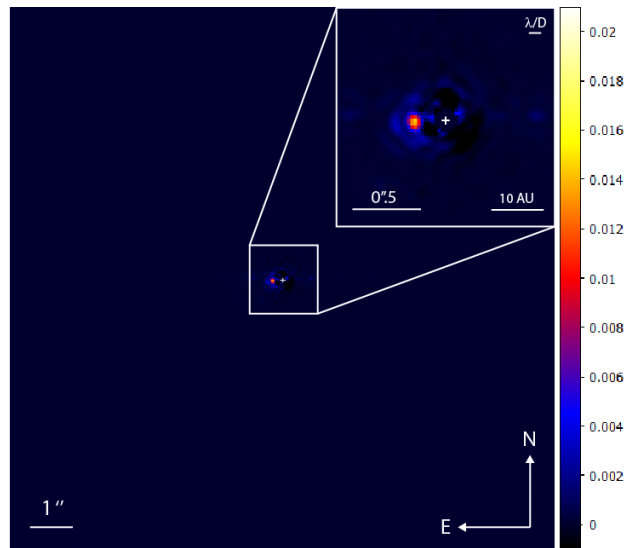


Figure 3: ϵ Cep final K_s -band reduced image after photometry calibration. The white cross indicates primary star position and the inner λ/D region is masked.

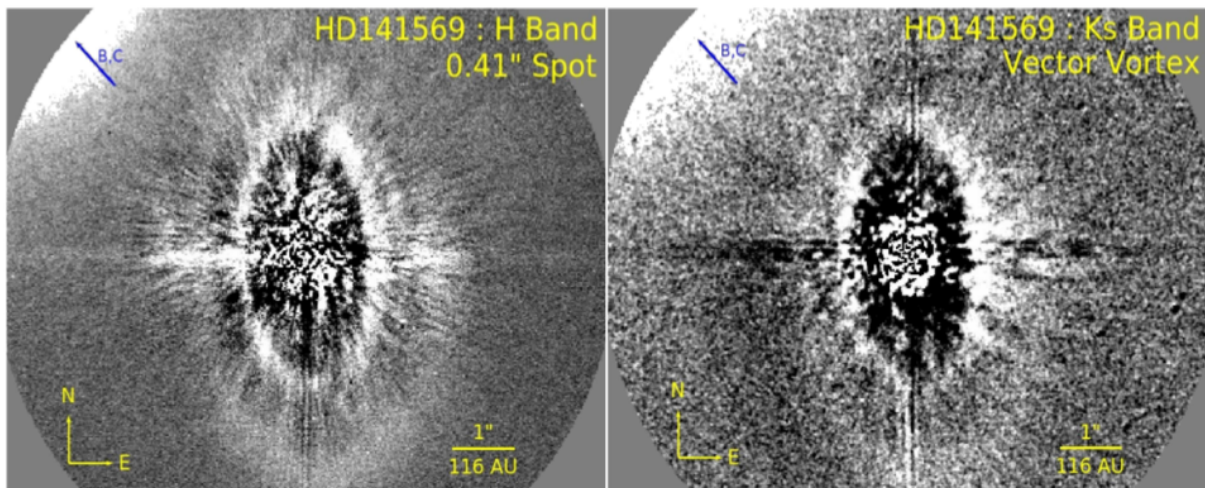


Figure 4: Comparison of the two images taken in H with a hard-edge mask (left), and Ks with the VVC (right). The flux in the north west of each image is coming from the PSF wings of HD 141569 B and C. The two known rings are visible in both images, however the structure between the rings east of the central star is only visible in the H band image.

We observe an inner clearing from $\sim 0.5''$ (50 AU) out to the edge of the inner disk at $1.77''$ (177 AU). The inner disk is $0.64''$ (64 AU) wide and extends out to $2.41''$ (241 AU). The outer disk has emission from $3.06''$ to $3.87''$ (306 to 387 AU) with a width of $0.81''$ (81 AU). Both are offset from the central star by a measurable amount, but do not share a common center. There is also an obvious gap between the two disks, which may be cleared by a forming exoplanet. The gap has alternatively been interpreted as part of a spiral structure formed from perturbations of B and C [8-10] whose PSF wings are visible in the North-West corner of Figure 4. There is an arc like structure between the two rings that has been associated to this spiral structure as well.

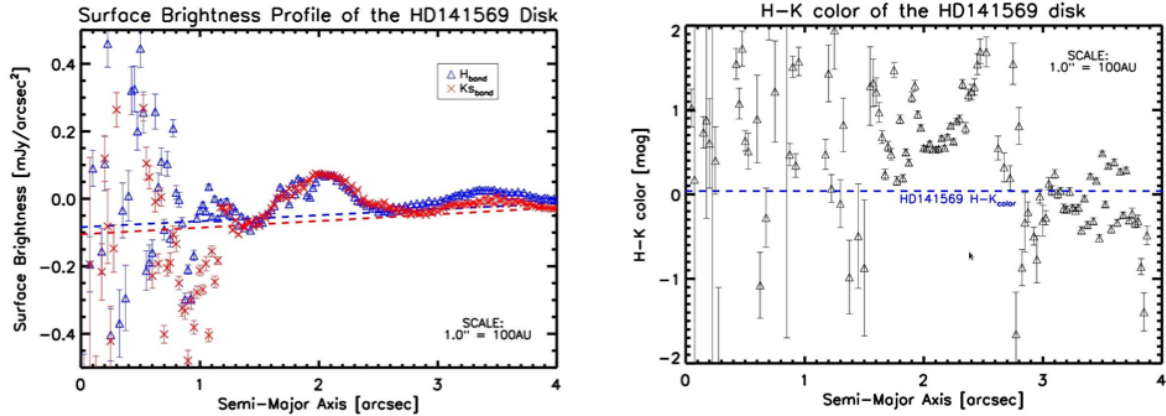


Figure 5: The plot on the left shows the surface brightness profiles for the two observations; in blue is the H band, and in red is the Ks band. Our data reduction with KLIP, while optimized for revealing the extended emission from the disk, incurs a dark hole of non-astrophysical negative residuals around the star. As a first-order attempt at removing this effect, we fit a line to the minimum residual emission as a function of radial separation (dashed blue and red lines). The profiles were created by integrating the flux in elliptical annuli concentric on the star and the colors were inferred from the corrected profiles.

The plots in Figure 5 show the H and Ks band surface brightness profiles of the HD 141569 disk (left) and the H-K disk color (right). The two peaks, one at $2.0''$, and the other, less prominent between $3.3''$ - $3.6''$ correspond to the mid-ring semi-major axes of the two circumstellar rings. Our data lose sensitivity inwards of $0.8''$, although for the first time we can rule out $> 3\times$ brighter rings inwards to $0.5''$. Another new result is the determination of the near-infrared color of the circumstellar disk. In particular, the outer ring is 0.5 - 1.0 mag bluer than the inner ring. This suggests that the outer ring may be dominated by smaller, sub-micron sized grains that are in the process of being blown out by radiation pressure.

3. P1640 Coronagraphy and Spectroscopy

Project 1640 is a suite of high contrast imaging instrumentation installed at Palomar Observatory [1, 11,12]. The primary science goal is to obtain images and low-resolution spectroscopy of substellar and planetary mass companions across the Y, J, and H-bands. Such information is already providing constraints on composition, temperatures, and surface gravities of planets and low-mass companions. The core of the instrumentation is an apodized-pupil Lyot coronagraph integrated with a microlens-based integral field spectrograph (IFS). This instrument ensemble is mounted on the PALM-3000 AO system, which in turn is mounted at the Cassegrain focus of the 200-inch Hale Telescope at Palomar. In addition, Project 1640 uses an internal wave front calibration interferometer [13,14] for reducing non-common path wave front errors internal to the instrument. This additional subcomponent has the effect of boosting performance at small angular separations (a few λ/D). In addition to obtaining low-resolution spectra, our broad wavelength coverage and ~ 19 milliarcsecond pixel scale allows suppression of the chromatically dependent speckle noise. This system is the first of a new generation of apodized-pupil Lyot coronagraphs combined with high-order adaptive optics and imaging spectrographs (e.g. GPI, SPHERE, SCExAO/CHARIS), and we anticipate that this instrument will

make a lasting contribution to high-contrast imaging in the Northern Hemisphere for years. In the following sections, we highlight several of the early science results to come out of the initial phases of this effort, including simultaneous spectroscopy of multiple planetary mass companions in the HR 8799 system, spectroscopy of several remarkable young binary systems, and information retrieved for the brown dwarf Kappa Andromedae B.

3.1. Spectroscopy of the HR8799 Star System

The HR 8799 system is the first exoplanetary solar system with multiple directly imaged planetary mass companions. This A5V star possesses a bright debris disk, and has an estimated age of 30 Myr, based on its co-moving status with several other members of the 30 Myr Columba stellar association.

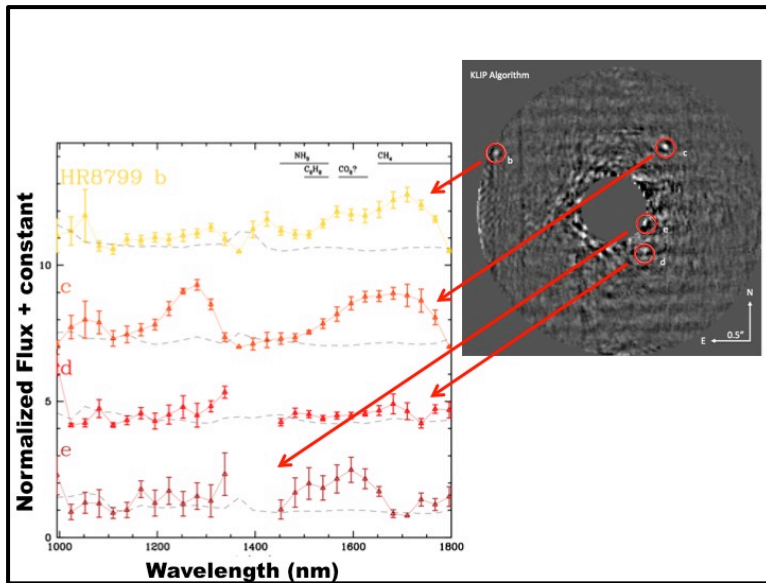


Figure 6: Simultaneous spectra of the four planetary mass companions associated with the HR 8799 systems obtained from Project 1640.

With Project 1640, we obtained spectra of all four planets at two epochs in 2012 giving the first simultaneous spectra of multiple planets orbiting another star (Figure 6). These results highlight the power of discerning spectral differences between planets in multi-planet systems, which can provide constraints on the formation locations for each object. Specifically, Oberg et al. [15] demonstrated that carbon-to-oxygen ratios in exoplanet atmospheres may constrain the formation locations of such objects, since various snow lines of carbon and oxygen-rich ices form at various radial locations from the star. Our study uses two independent methods for speckle suppression, and in Oppenheimer et al. [16], we demonstrate that these two methods return remarkably similar spectra. Further, our spectra agree well with previously existing H-band spectra of the HR 8799 b companion [17].

3.2. FU Orionis

During the initial phase of the Project 1640 data collection, as well as during commissioning, the Project 1640 science goals were partly geared toward binary star characterization, and particularly to analyzing young binary systems. Here we briefly highlight some of these results.

FU Orionis, the prototypical very young star after which the broader class of objects is named, was an early target for Project 1640. FU Ori is a binary system with a fainter, stellar companion discovered nearly a decade ago, located 0.4 arcseconds south of the primary. A body of evidence gathered over the last decade is consistent with the companion “FU Ori S” being a young, low-mass, perhaps K-type, T-Tauri star. In an effort to further elucidate the nature of FU Ori S by quantifying the spectral type and the reddening, and to assist in interpretation of the dust shell encircling the FU Ori N/S system, we observed this source with Project 1640. Figure 7 shows our image and spectra, and our results are presented in Pueyo et al. [18]. We briefly highlight the major science results here.

Combining our J and H-band spectrophotometry of the FU Ori S member, previously published K-band spectra, as well as L- and N-band photometry allowed us to fit an SED model with blackbody effective temperatures and interstellar reddening as inputs. The companion FU Ori S appears to be the much more heavily reddened ($A_v = 8-12$) member of the system, and perhaps even slightly hotter (4000-

6500K). Hence, this analysis reveals that FU Ori S is thus much more massive than previously believed and, with a lower bound for the mass estimate ($> 0.5 M_{\text{solar}}$), it is the most massive component of this system.

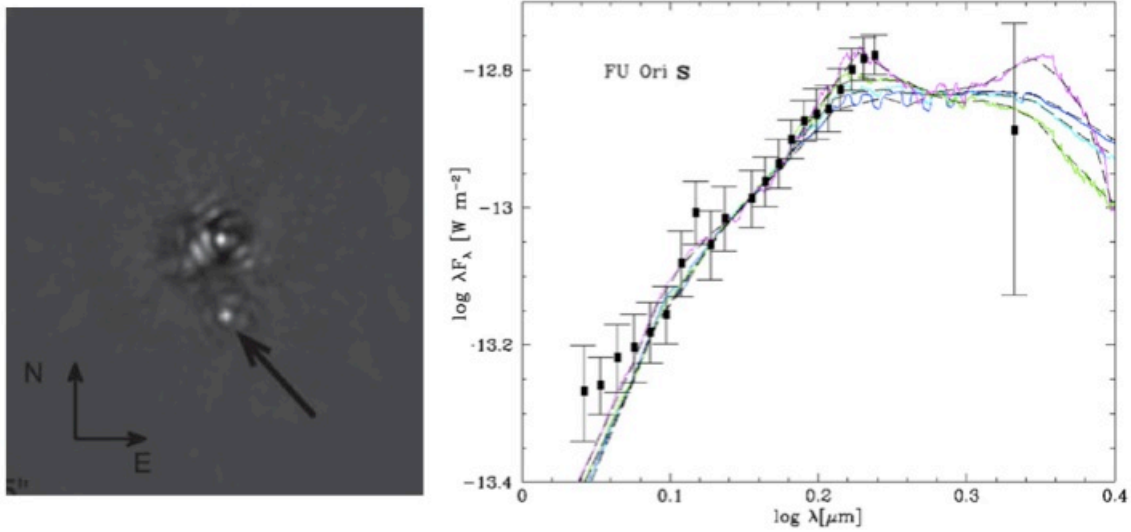


Figure 7: Project 1640 images and spectra of the prototypical young binary system FU Orionis. *Left:* the image shows the star coronagraphically occulted with the binary companion 0.4 arcseconds to the south. *Right:* the Project 1640 spectrum in the J and H-bands as well as a K-band photometric point taken from the literature. Model fitting of reddened SEDs indicate this companion is the more massive member.

3.3. Z Canis Majoris

The Z Canis Majoris system (“Z CMa”) is a remarkable young (< 1 Myr) binary system that was one of the original members of the set of Ae and Be stars with strong nebulosity first identified nearly 50 years ago. Along with strong P Cyg profiles in the Balmer lines, radio continuum emission, bipolar jets as well as a strong infrared excess, the high level of photometric variability of this system has been tracked for decades, showing periodic outbursts common to FU Ori type objects. Combining decades of information on this object, a physically consistent picture of this system has emerged revealing that Z CMa is comprised of an FU Ori-like object and Herbig Ae/Be object with separation of ~ 100 AU. At such a large distance (1150 pc), the separation of the binary pair spans only 1-2 diffraction widths (~ 100 mas), and the true nature of this remarkable system has only started to become clear with the advent of high angular resolution imaging on large 5-10m telescopes.

Z CMa was observed by Project 1640 in March 2009, during the 2009 outburst [19]. In Figure 8 we show three images taken at three different wavelengths spanning the J and H-bands. The superior AO correction provided by PALM-3000 allowed us to verify that the Herbig Ae/Be component was solely responsible for the continuum brightness doubling associated with the 2009 outburst. In addition, adding to our analysis K and L-band (2.2 and 3.8 micron) photometry taken close in time at the W. M. Keck Observatory allowed us to fit reddened two-component blackbody models to the data. The two-component models roughly correspond to a photosphere and disk component, although we refrain from assigning too much physical meaning to this simple model. Regardless, in this regime, we derive temperatures of 8500K and 5500K for the Herbig Ae/Be member and FU Ori member, respectively. At the same time, our model fitting provides temperatures of 1100K and 900K for the disk components of the Herbig and FU Ori members.

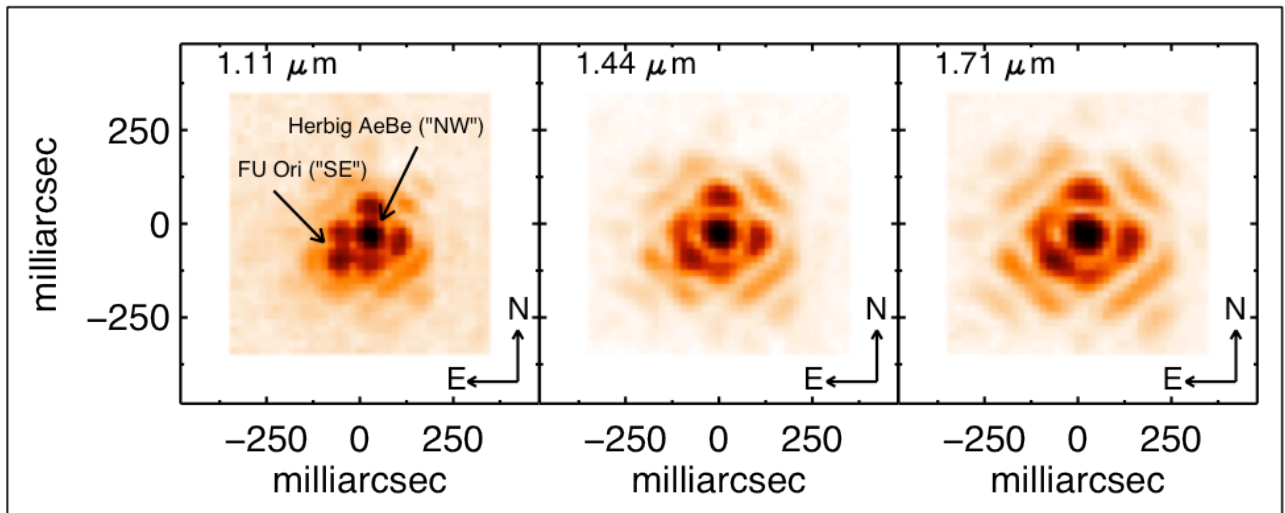


Figure 8: Three images of the Z Canis Majoris system at 1.11, 1.44, and 1.71 mm from Project 1640 taken during outburst. The combination of AO correction and multispectral imaging demonstrates conclusively that the Herbig Ae/Be member is responsible for the outburst.

3.4. Kappa Andromedae

Kappa Andromedae is a B9IV star at 52 pc for which a faint companion separated by 55 AU (~ 1 arcsecond) was recently announced [4]. In December 2012, this object was observed by Project 1640 obtaining a clear detection of the companion (See Figure 9) as well as a spectrum in the Y, J, and H-bands (See Figure 10 below). While the detection in the Y-band was lower signal-to-noise, the H-band detection was a factor of several above the detection limit. Comparison of our low-resolution spectra to empirical, higher-resolution brown dwarf spectra show similarities with low-gravity mid L-dwarfs, but similarities with late L-type field objects are also present. Fitting synthetic spectra from PHOENIX model atmospheres [20] the Project 1640 spectrum suggests an effective temperature of ~ 1800 K and a surface gravity, $\log(g)$, closer to that of field age objects (~ 5.1 - 5.3) rather than to the young 30 Myr age reported previously. This interpretation is corroborated by several independent lines of evidence suggesting that the host star Kappa Andromeda A is significantly older (~ 200 Myr) than the 30 Myr initially proposed (Hinkley et al. *in prep*). Our spectroscopic evidence combined with our re-assessment of the system age implies a substellar companion mass of ~ 50 - 70 Jupiter masses, consistent with a brown dwarf rather than a planetary mass companion.

Further, our spectrum of the Kappa Andromedae system demonstrates the power in obtaining multi-wavelength high resolution images with dedicated exoplanet imaging platforms. Even with relatively modest spectral resolutions ($R \sim 45$), powerful constraints on the temperatures and gravities for substellar objects can be obtained when compared with theoretical spectral models.

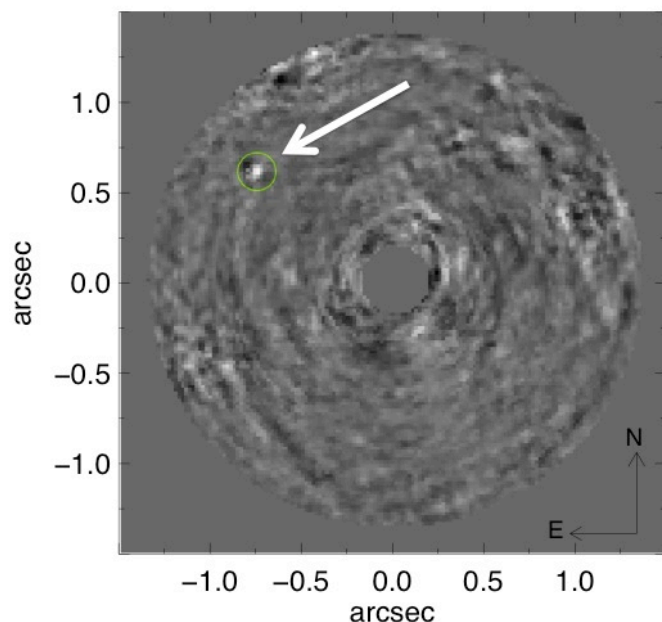


Figure 9: A post-processed image obtained in December 2013 from the Project 1640 high contrast imaging platform showing the Kappa Andromedae B companion at the upper left.

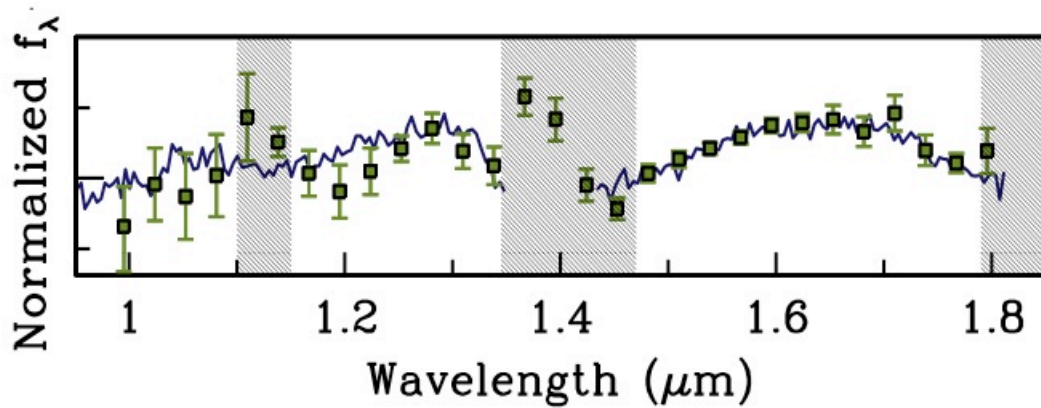


Figure 10: The spectrum of the companion to Kappa Andromedae (points) obtained from the Project 1640 high contrast imaging spectrograph. Overlaid on this spectrum is a higher resolution spectrum of a “standard” late-L dwarf taken from Kirkpatrick et al. [21].

4. Acknowledgements

This work was carried out at the Jet Propulsion Laboratory, California Institute of Technology, under contract with the National Aeronautics and Space Administration, and is based on observations obtained at the Hale Telescope, Palomar Observatory, as part of a continuing collaboration between the California Institute of Technology, NASA/JPL, Stony Brook University, and the American Museum of Natural History. We thank the staff of the Palomar Observatory for their continued support.

Reference herein to any specific commercial product, process, or service by trade name, trademark, manufacturer, or otherwise, does not constitute or imply its endorsement by the United States Government or the Jet Propulsion Laboratory, California Institute of Technology.

5. References

- [1] Dekany, R. *et al.*, PALM-3000 : Exoplanet adaptive optics for the 5-meter Hale Telescope. *The Astrophysical Journal* **xxx**, ppxxxx-xxxx (2013)
- [2] Mawet, D. *et al.*, Optical Vectorial Vortex Coronagraphs using Liquid Crystal Polymers: theory, manufacturing and laboratory demonstration. *Opt Express* **17**, 1902-1918 (2009)
- [3] Serabyn, E., Mawet, D. & Burruss, R., An image of an exoplanet separated by two diffraction beamwidths from a star. *Nature* **464**, 1018-1020, doi:Doi.10.1038/Nature09007 (2010).
- [4] Carson, J. *et al.*, Direct Imaging Discovery of a "Super-Jupiter" around the Late B-type Star κ And. *The Astrophysical Journal Letters* **763**, L32 (2013).
- [5] Soummer, R. *et al.*, Detection and Characterization of Exoplanets and Disks Using Projections on Karhunen-Loève Eigenimages. *The Astrophysical Journal Letters* **755**, L28 (2012).
- [6] Mawet, D., Mennesson, B., Serabyn, E., Stapelfeldt, K. & Absil, O. A Dim Candidate Companion to epsilon Cephei. *The Astrophysical Journal Letters* **738**, L12 (2011).
- [7] Van Leeuwen, F., Validation of the New Hipparcos Reduction. *Astronomy and Astrophysics*, **474**, 653-664 (2007).
- [8] Clampin, M. *et al.*, ACS Coronagraphic Observations of Optically Thin Debris Disks. International Astronomical Union Symposium **221**, 449 (2003).
- [9] Quillen, A.C. *et al.*, Driving spiral arms in the circumstellar disks of HD 100546 and HD 141569A. *The Astronomical Journal* **129** 2481-2495 (2005).
- [10] Ardila, D.R. *et al.*, A Dynamical Simulation of the Debris Disk Around HD 141569A. *The Astrophysical Journal* **627** 986-1000 (2005).
- [11] Hinkley, S. *et al.*, A new high contrast imaging program at Palomar observatory. Publications of the Astronomical Society of the Pacific **123**, 74-86 (2011).

- [12] Oppenheimer, B.R. *et al.*, Project 1640: The World's First Extreme-AO Exoplanet Imager. Proceedings of the SPIE **8447**, 844720-1 (2012)
- [13] Wallace, J.K. *et al.* Science camera calibration for extreme adaptive optics. Proceedings of the SPIE **5490**, 370-378 (2004).
- [14] Zhai, C. *et al.*, First Order Wavefront Estimation Algorithm for P1640 Calibrator. Proceedings of the SPIE **8447**, 84476W (2012).
- [15] Oberg, K.I. *et al.*, The effects of snowlines on C/O in planetary atmospheres. *The Astrophysical Journal Letters* **743**, L16 (2011).
- [16] Oppenheimer, B.R. *et al.*, Reconnaissance of the HR 8799 Exosolar System I: Near IR Spectroscopy. *The Astrophysical Journal* **768**, 24 (2013).
- [17] Barman, T. *et al.*, Clouds and Chemistry in the Atmosphere of Extrasolar Planet HR8799b. *The Astrophysical Journal* **733**, 65 (2011).
- [18] Pueyo, L. *et al.*, Constraining mass ratio and extinction in the FU Orionis binary system with infrared integral field spectroscopy. *The Astrophysical Journal* **757**, 57 (2012).
- [19] Hinkley, S. *et al.*, High-resolution Infrared Imaging and Spectroscopy of the Z Canis Majoris System during Quiescence and Outburst. *The Astrophysical Journal Letters* **763**, L9 (2013).
- [20] Allard, F. *et al.*, The limiting effects of dust in brown dwarf model atmospheres. *The Astrophysical Journal* **556**, 357 (2001).
- [21] Kirkpatrick, J.D. *et al.* Discoveries from a near-infrared proper motion survey using multi-epoch Two Micron All-Sky Survey data. *The Astrophysical Journal Supplement* **190**, 100 (2010).